

High-Energy Electron Exposure Testing of Traveling-Wave-Tube Amplifiers

Alexander Bogorad,* Herbert Wolkstein,† and Roman Herschitz‡
Lockheed Martin Corporation, Newtown, Pennsylvania 18940

The exposure of traveling wave tubes (TWT) to a high-energy electron environment, typical of the space environment experienced by commercial communications spacecraft in geosynchronous orbit during a 15-yr mission, is discussed. It is shown that no changes in the performance of both Ku-band and C-band traveling wave tubes were observed as a result of exposure to high-energy electrons. These traveling wave tubes therefore can meet service life requirements and can be flown in the proposed location outside the spacecraft structure without the necessity of adding additional radiation shielding to the TWT or the high-voltage cable.

Introduction

RECENTLY, because of the increase of downlink channels, the payload component layout on several commercial communications programs required mounting traveling wave tubes (TWTs) outside the spacecraft structure. In this location they are shielded on one side by only thermal blankets. On all previous spacecraft the TWTs were mounted inside the spacecraft structure where they were shielded by metallic spacecraft panels. However, as the size of the payload increases, placement of the TWTs outside the spacecraft structure becomes desirable. A typical communications spacecraft and the proposed TWT location are shown in Fig. 1. In this location TWTs are exposed to high fluxes of energetic electrons and an exceedingly large total dose of ionizing radiation. This radiation is naturally occurring and is present at different levels on all spacecraft orbits. It is associated with solar activity and is extensively investigated by a number of NASA and military missions.¹ Radiation ejected from the sun interacts with the Earth's magnetic environment. Most of the radiation is deflected by the Earth's magnetic fields. Some radiation, however, gets injected through the auroral regions and the magnetotail on the dark side of the Earth. Consequently, some radiation gets trapped, causing complex processes of interaction including auroras, magnetic storms, electromagnetic waves, etc.² These interactions create a constant radiation background levels that primarily include electrons and protons. This radiation level and fluxes of charged particles vary as a function of altitude and orbit.^{3–5} In addition, during solar proton events, the fluxes of electrons and protons increase temporarily by several orders of magnitude for the duration of the event (1–4 days).

High-energy electrons can penetrate TWT housing and high-voltage (HV) cable shields and collect at various internal components of TWTs, such as on dielectrics in the electron gun, anode and cathode areas, and the dielectric supports in the helix regions. This electron charging, in turn, could result in TWT defocusing and in electrostatic discharges causing TWT amplifier (TWTA) spontaneous shut off or it could impact TWT performance in other ways. Furthermore, total dose accumulation could degrade dielectric properties of the HV cable and other dielectric inside the TWT. These effects were frequently observed on other spacecraft components.^{5–7} The electronic power conditioner (EPC), normally integrated with its companion TWT, has been shielded and, therefore, excluded from these tests.

A series of tests was performed to verify that TWT operation is not affected by such increased exposure over a typical 15-yr geosyn-

chronous mission. Tests were performed at the Linear Accelerator Facility (LINAC) at the University of Maryland by exposing two typical TWTs to an equivalent 15-yr electron fluence. In this paper we have considered electron energies of greater than 0.5 MeV because electrons with lower energies will not penetrate through the 6-mil thermal blanket and TWT 20-mil-thick housing or HV cable braid shield. The exposure flux was derived from measurements made in geosynchronous orbit by Los Alamos spacecraft during May 1992. This is considered worst-case geosynchronous charging environment. In addition, total exposure was derived from AE8-Max NASA Goddard Space Flight Center model.

Instrumentation and the Test Articles

The TWTs subjected to this series of simulated orbital environmental tests included a 55-W AEG C-band TWT (type TL-4059) and an AEG 135-W Ku-band TWT (type TL-12135). The C-band TWT was designed to operate over the 3.6–4.2-GHz frequency band, whereas the Ku-band TWT was designed to operate over the 11.7–12.2 GHz band. The salient operating features of these two types of metal-ceramic, periodically focused TWTs are listed in Table 1.

The specific operating voltages for both of these TWT types are listed in Table 2. As indicated, the C-band TWT has a helix-to-cathode potential of 3490 V, whereas the Ku-band TWT operates with helix-to-cathode potential of 5960 V. The C-band TWT was tested with a 36-in.-long HV Gore cable, whereas the Ku-band TWT was tested with a 12-in.-long Gore cable. The cables were used to interconnect each TWT to its integrated power supply.

This Gore HV cable consists of nine separate HV leads. Each lead consists of six twisted strands of AWG26 gauge copper wire, which is covered with Teflon[®] insulation. HV cable is also overwrapped with a double-braid metal shield composed of 36,010 AWG wire (~12 mil of Ni plated copper) with approximately 90% coverage. This type of braid provides equivalent radiation shielding of approximately 80-mil equivalent aluminum.

TWT housing is made from the combination of stainless steel, magnesium (Mg), and aluminum (Al) alloys with a thickness of approximately 20 mil or greater. Test articles also included flight-type aluminum input RF cables, which can charge and possibly degrade as a result of the exposure to high-energy electron environment.

Test Setup and Test Procedure

TWTs were mounted on a 0.635-cm-thick aluminum plate such that TWT, HV, and RF cables were all exposed to the electron beam. Associated power supplies were mounted on the back of the plate; thus, they were shielded from the electron beam. This mounting configuration is consistent with the flight configuration where these power supplies are mounted inside the spacecraft and are not exposed to the higher external flux. A block diagram of the test setup is shown in Fig. 2.

The TWTA power, command, and telemetry harness was connected to the special test equipment and computer control data collection system (CCDC) located outside the radiation area. The

Received 24 February 2000; revision received 23 June 2000; accepted for publication 26 June 2000. Copyright © 2000 by the American Institute of Aeronautics and Astronautics, Inc. All rights reserved.

*Senior Staff Engineer, Communications and Power Center, 100 Campus Drive.

†Consultant, Communications and Power Center, 100 Campus Drive.

‡Manager of Survivability Engineering Group, Communications and Power Center, 100 Campus Drive. Senior Member AIAA.

CCDC system was used to automatically and continuously monitor, record, and store the TWTA telemetry throughout the duration of the test. Telemetry data were collected and recorded every 10 s. A block diagram of the CCDC is shown in Fig. 3. Figure 4 shows a flowchart of the software that was written to operate the CCDC system and collect the test data. The values of helix current (I_{helix}), RF power, and bus current (I_{bus}) were continuously recorded throughout the test. All other telemetry (including anode voltage telemetry) was

manually recorded periodically during the test. TWT was operated at saturated drive during the test.

The following is a brief summary of the test procedure:

1) Prior to exposing TWTs to the electron beam, both units were operated in the saturated drive mode continuously for 15 h, and the telemetry was recorded to establish the pretest baseline. In the saturated mode the TWT is operated with suppressed RF input drive to obtain maximum RF output power. During this mode of operation, the TWTs were subjected to the following environments.

2) Units were exposed for 6 h to the electron beam with energy $E = 0.5 \text{ MeV}$ and current density $J = 10 \text{ nA/cm}^2$ (total fluence $f = 1.4 \times 10^{15} \text{ electrons/cm}^2$).

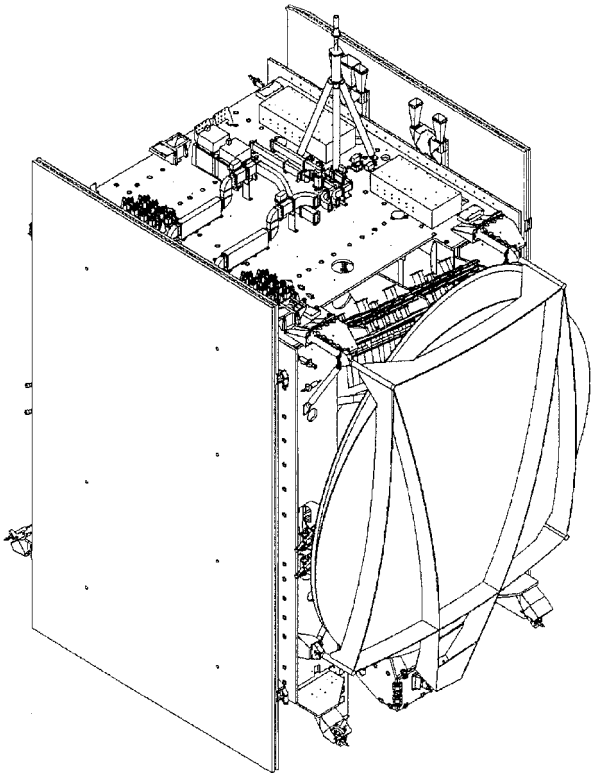


Fig. 1 Typical communication spacecraft.

Table 1 Conduction-cooled TWT test vehicles nominal parameters

Operating band	C-band	Ku-band
TWT type	TL-4059	TL-12135
Frequency	3.6–4.2 GHz	11.7–12.2 GHz
Nominal output power	55 W	135 W
Efficiency	57%	64%
Gain	53 dB	55 dB
Nonlinear phase	40 deg	40 deg
Helix potential	3500 V	6000 V
Cathode current	60 mA	90 mA
RF couplers-input	SMA	SMA
RF coupler-output	TNC	Waveguide WR-75

Table 2 Typical TWT operating potentials

Electrode	C-band, V	Ku-band, V
Filament	4.52	4.49
Helix (Gnd)	3490	5960
Anode	3160	5490
Coll #1	1980	3230
Coll #2	1580	2473
Coll #3	790	1192
Coll #4	0 (–3490) Rel to Gnd	0 (–5960) Rel to Gnd

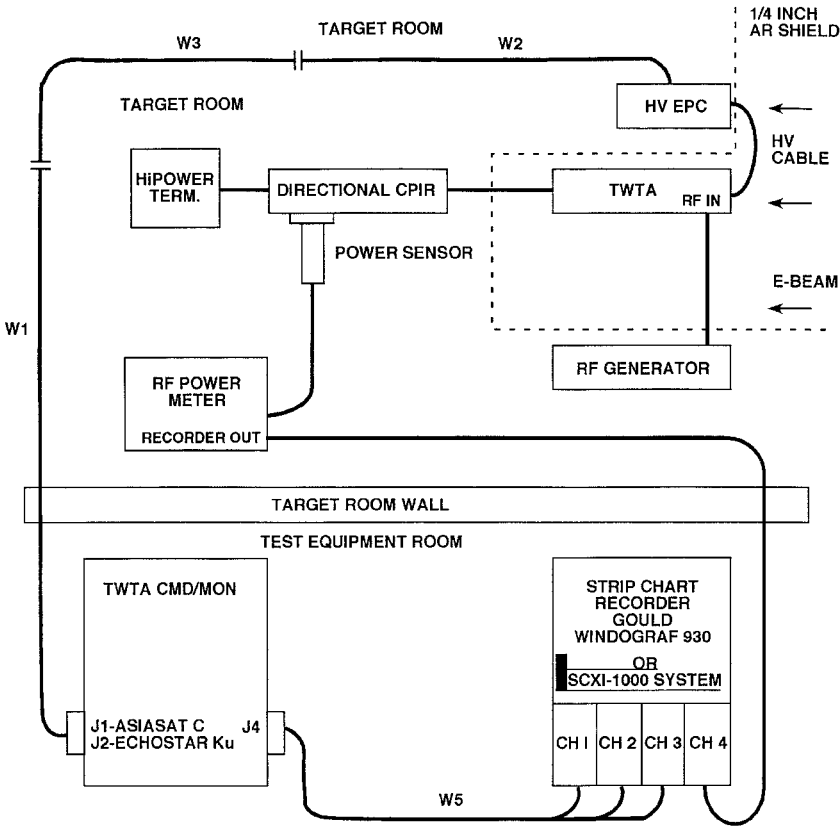


Fig. 2 TWTA test setup.

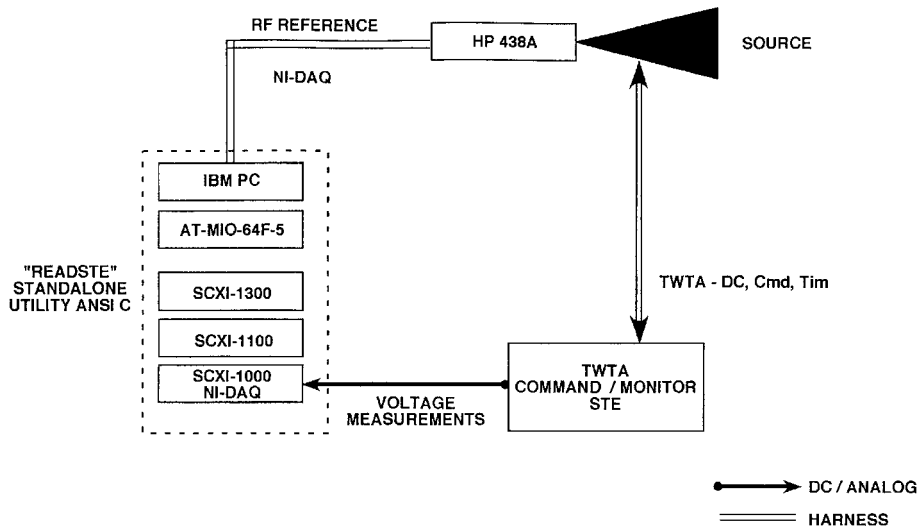


Fig. 3 TWTA digital command, dc measurements, and dc control.

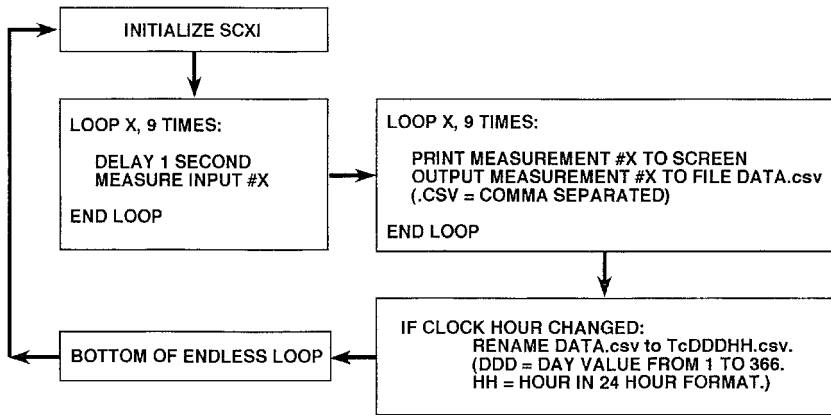


Fig. 4 Software flowchart.

3) Next, the units were exposed for 6 h to the electron beam with energy $E = 2$ MeV and current density $J = 1.5$ nA/cm² (total fluence $f = 2.0 \times 10^{14}$ electrons/cm²).

4) Then, the units were exposed for 6 h to the electron beam with energy $E = 4$ MeV and current density $J = 0.05$ nA/cm² (total fluence $f = 6.8 \times 10^{12}$ electrons/cm²).

5) Finally, the units were exposed for 2 h to the electron beam with energy $E = 6$ MeV and current density $J = 0.05$ nA/cm² (total fluence $f = 2.3 \times 10^{12}$ electrons/cm²).

The LINAC electron beam at the University of Maryland has a Gaussian energy distribution, which is 1 MeV wide at full width at half-maximum (FWHM).

Exposure Levels and Space Radiation Environment

Table 3 summarizes radiation dose requirements for a typical commercial communications satellite in geosynchronous (GEO) orbit. This dose consists of the electron fluence of greater than 0.5 MeV that occurred during the May 1992 Solar Flare, a total 15-yr mission electron fluence, as well as test-level fluence. Electron energies of greater than 0.5 MeV were selected for the test because electrons with lower energies will not penetrate through the 6-mil thermal blanket and 20-mil-thick TWT housing or HV cable-braid shield.

Table 3 shows that during the test TWTs were exposed to total electron fluence that is two to three orders of magnitude higher than worst-case fluence expected during anomalously large solar flare. This environment could cause electrostatic discharges on the TWT dielectric components. Should TWT be found immune to this worst-case levels, it would conclusively demonstrate that it is immune to the effects of the internal charging.

Table 3 On-orbit and test radiation environment

Energy, MeV	1992 flare fluence ^a	15-yr fluence	Test fluence
0.5-1	1.0×10^{12}	1.0×10^{15}	1.4×10^{15}
1-3	7.7×10^{11}	1.9×10^{14}	2.0×10^{14}
3-5	4.5×10^{10}	1.4×10^{12}	6.8×10^{12}
>5	5.5×10^9	1.5×10^9	2.3×10^{12}

^aAssuming 24-h flare duration; fluence is in e⁻/cm².

Furthermore, the test electron fluence is equal to or higher than the total dose experienced by typical spacecraft electronics on commercial communications satellite in GEO orbit. Should the TWT be found immune to these worst-case levels, such a result would conclusively demonstrate that it is immune to the total dose effects, which are typical spacecraft will experience during 15-yr mission. Consequently, the test fluence represents the worst-case internal charging as well as a total dose environment for TWTs in their proposed location.

Results

Test results are summarized in Figs. 5 and 6. These figures and tables show 1-h average telemetry plots for Ku- and C-band TWTAs. TWT A telemetry data for a preexposure 15-h run are plotted as a function of time. Figure 5a shows telemetry data for Ku-band TWT A, and Fig. 6a shows telemetry data for C-band TWT A. The data indicate that no performance degradation occurred in either of the tubes during a 15-h preexposure test run. Figure 5b shows Ku-band telemetry plots as a function of time during the TWT A

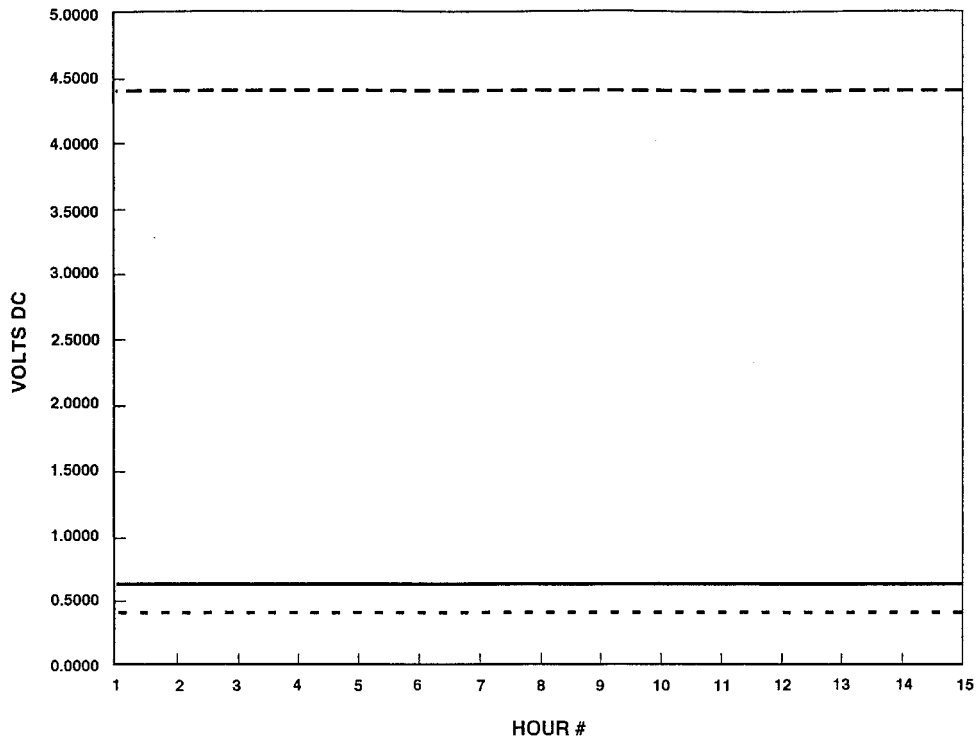


Fig. 5a Ku-band pretest telemetry: ---, Ku-band IBus tlm; —, Ku-band RF power; and - . - ., Ku-band helix tlm.

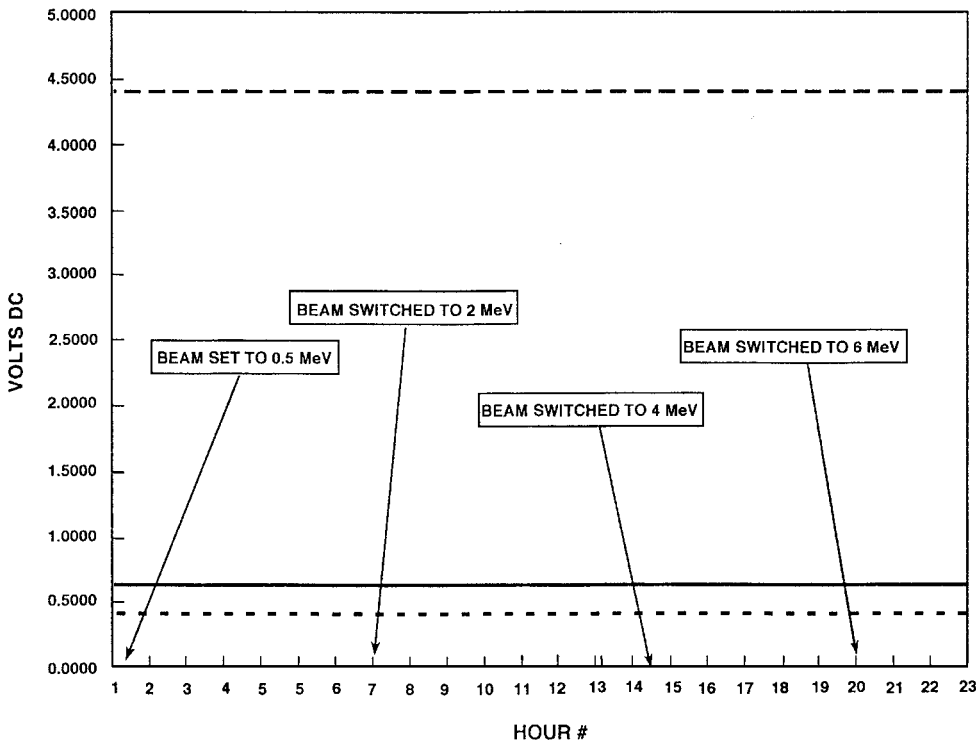


Fig. 5b Ku-band telemetry during electron beam irradiation: —, Ku-band RF power; ---, Ku-band IBus tlm; and - . - ., Ku-band helix tlm.

exposure to a high-energy electron beam. Figure 6b shows C-band telemetry plots as a function of time during the TWTA exposure to a high-energy electron beam. The telemetry data indicate that no performance degradation occurred in either of the tubes as a result of 24-h exposure to a high-energy electron beam. Telemetry data for both TWTA's were collected every 10 s throughout the test.

Furthermore, no changes were observed in anode voltage telemetry for either TWT. Anode telemetry for Ku-band TWTA prior and following the exposure was 4.90 and 4.91 V, respectively. Anode

telemetry for C-band TWTA prior to and following the exposure was 3.10 and 3.10 V, respectively.

Conclusions

Review of the data shows no changes in any of Ku-band or C-band TWTA telemetry readings as a result of the exposure to high-energy electrons. The test exposure levels were at least a factor of 100 more severe than that expected from the worst-case solar flare internal charging environment, and total dose exposure levels were representative of a 15-yr geosynchronous mission on a typical

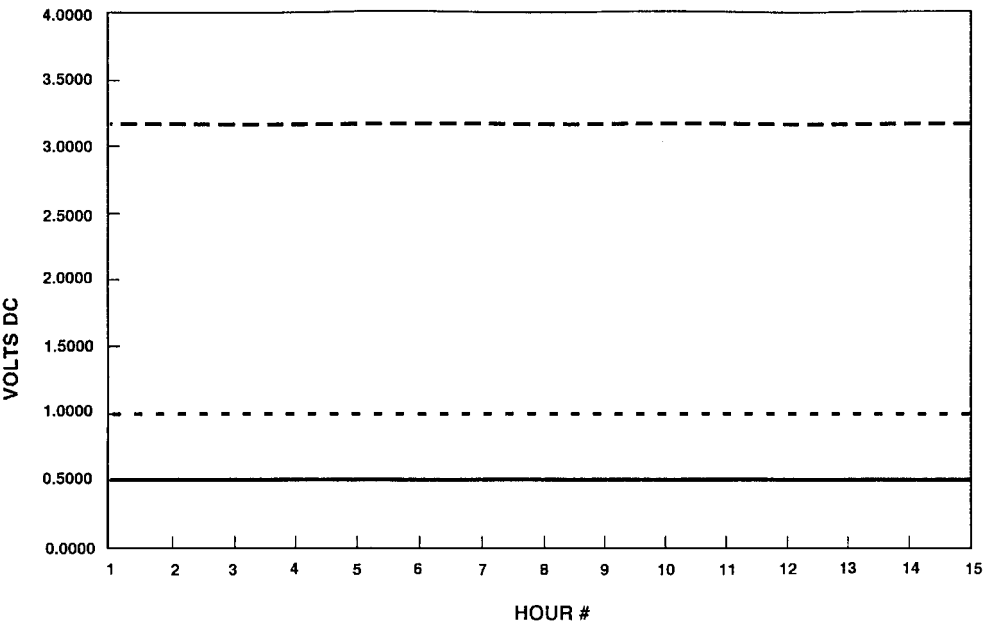


Fig. 6a C-band pretest telemetry: ---, C-band IBus tlm; - - -, C-band helix tlm; and —, C-band RF power.

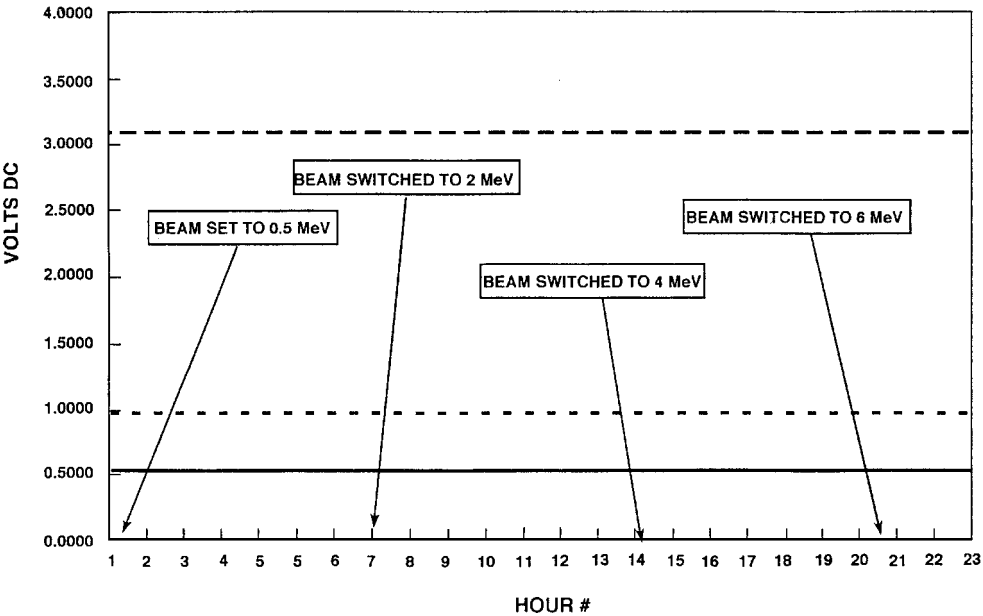


Fig. 6b C-band telemetry during electron beam irradiation: —, C-band RF power; ---, C-band IBus tlm; and - - -, C-band helix tlm.

commercial communication satellite. Therefore, test results confirm that the TWTs which were tested and other TWTs of similar construction are not susceptible to internal charging or total dose radiation effects.

References

¹Drooling, D., "Stormy Weather in Space," *IEEE Spectrum*, Vol. 32, No. 6, 1995, p. 64.
²Hekkila, W. J., "Outline of Magnetosphere Theory," *Journal of Geophysics Research*, Vol. 79, No. 16, 1974, p. 2496.
³Benedetto, J., "Economy-Class Ion-Defying ICs in Orbit," *IEEE Spectrum*, Vol. 35, No. 3, 1998, pp. 36-41.

⁴Hasting, D., and Garrett, H., *Spacecraft Environmental Interaction*, Cambridge Univ. Press, Cambridge, England, U.K., 1996, pp. 229-232.
⁵Gombosi, T. I., *Physics of the Space Environment*, Cambridge Univ. Press, Cambridge, England, U.K., 1998, pp. 265-272.
⁶Fredereckson, A. R., "Methods for Estimating Spontaneous Pulse Rate for Insulators Inside the Spacecraft," *IEEE Transactions on Nuclear Science*, Vol. 43, No. 6, 1996, pp. 2778-2782.
⁷Wrenn, G., and Smith, R., "Probability Factors Governing ESD Effects in Geosynchronous Orbit," *IEEE Transactions on Nuclear Science*, Vol. 43, No. 6, 1996, pp. 2783-2789.

A. C. Tribble
Associate Editor